

Fluorescence Probe Techniques (FPT) for Measuring the Relative Efficiencies of Free-Radical Photoinitiators

Shengkui Hu, Roman Popielarz, and Douglas C. Neckers*

Center for Photochemical Sciences, Bowling Green State University, Bowling Green, Ohio 43403,¹ and Spectra Group Limited, Inc., 1722 Indianwood Circle, Suite H, Maumee, Ohio 43537

Received September 22, 1997; Revised Manuscript Received April 13, 1998

ABSTRACT: A new method for determining the relative efficiencies of free-radical photoinitiators is reported. Called the fluorescence probe technique (FPT), the method has been used to determine the relative initiation efficiencies of several commercial photoinitiators and new phenyl glyoxylate derivatives in the photopolymerization of a model monomer, triethylene glycol diacrylate. The reactivity of each initiator was measured in reference to that of a standard commercial initiator, 2,2-dimethoxy-2-phenylacetophenone, Irgacure 651. Efficiencies differ widely among the acetophenone derivatives studied, and the phenylglyoxylate initiators are somewhat less reactive than the standard.

Introduction

Radiation cure technology has found a number of industrial applications because it is fast, efficient, and solvent-free.² The efficiency of the curing process is an important aspect of any working system, and this, in turn, is dependent on the initiating species. An easy measure of the reactivities of different photoinitiators would facilitate selection of initiators to achieve designated product properties, as well as establish, from structure–reactivity relationships, pathways to better initiators.

Various spectroscopic methods have been employed for the comparison of photoinitiator efficiencies. The most common are real-time infrared (RTIR) spectroscopy,³ Raman spectroscopy,⁴ Fourier transform IR spectroscopy,⁵ and nuclear magnetic resonance (NMR) spectroscopy.^{6,7} Other methods, such as photoacoustic,⁸ photocalorimetric,⁹ microwave dielectric,¹⁰ and holographic¹¹ measurements, are also occasionally employed. Recently, the use of fluorescent molecular probes for following polymerization progress in thin photocurable coatings has been reported. This method is based on the change of the fluorescence of a molecule (probe or dopant) resulting from a change in the viscosity of its immediate microenvironment.¹² Polymerization processes, in most cases going from liquid monomer to glassy solid, cause large changes in the mobility of the medium. Compounds whose fluorescence is sensitive to such changes can be used as indicators of the degree of polymerization. We have developed a number of different probes for following photopolymerization processes,¹³ including excimer-forming probes,¹⁴ twisted intramolecular charge-transfer (TICT) probes,¹⁵ and charge-transfer probes.¹⁶ The fluorescence spectrum of each exhibits pronounced blue shifts when the resins in which they reside are polymerized. However, the mechanism that causes the blue shift is fundamentally different among different types of probes. 5-(Dimethylamino)naphthalene-1-sulfonyl-*n*-butylamide (DASB), a typical TICT probe, has been employed in this study. Instrumentation dedicated for monitoring the polymerization process in situ has been developed.¹⁷

In this paper, we report a routine method for determining the relative initiation efficiencies (or relative

quantum yield of initiation) of photoinitiators based on fluorescence probe technology¹² called the fluorescence probe technique or FPT method. Results obtained using this method to evaluate the efficiencies of several commercial initiators as well as several new photoinitiators are reported. Quantum yields of initiation of several initiators for polymerization of a standard monomer were measured relative to Irgacure 651. Several acetophenone derivatives, which are common commercial initiators, and phenylglyoxylate esters which are new compounds were evaluated (Table 1).¹⁸

Experimental Part

Triethylene glycol diacrylate (TEGDA) was purchased from Sartomer and used as received. Irgacure and Darocure initiators (from Ciba-Geigy), methyl phenylglyoxylate (MPG) and ethyl phenylglyoxylate (EPG) (from Aldrich) were used without further purification. The syntheses of 2-chloroethyl phenylglyoxylate (CEPG), 2-bromoethyl phenylglyoxylate (BEPG), 2-(phenylthio)ethyl phenylglyoxylate (SEPG), and 2-ethoxyethyl phenylglyoxylate (EEPG) have been reported.¹⁹ 5-(Dimethylamino)naphthalene-1-sulfonyl-*n*-butylamide (DASB) is available from earlier studies.¹²

UV–visible spectra were obtained using an HP 8452 diode array spectrophotometer. NMR spectra were taken with either a Varian Gemini 200 NMR spectrometer or a Varian Unity Plus 400 NMR spectrometer using chloroform-*d* as the solvent. Chemical shifts are in ppm with TMS as the internal standard. GC/MS were taken on a Hewlett-Packard 5988 mass spectrometer coupled to an HP 5880A GC with a 30 m × 0.25 mm i.d. × 0.25 μm film thickness DB-5 MS column (J&B Scientific), interfaced to an HP 2623A data processor. Thin-layer chromatography was performed with Whatman silica gel coating TLC plates. Silica gel (60 Å, 60–200 mesh) used in column chromatography was from J. T. Baker Chemical Co. High-resolution mass spectra were obtained from University of Illinois at Urbana–Champaign.

Phenyl phenylglyoxylate (PPG) and ethyl glycol phenylglyoxylate (EGPG) were prepared by a general esterification protocol employing 1,3-dicyclohexylcarbodiimide (DCC).¹⁹ Spectroscopic data for PPG: ¹H NMR (400 MHz, CDCl₃) δ (ppm) 7.26–7.29 (m, 2H), 7.30–7.33 (m, 1H), 7.43–7.47 (m, 2H), 7.53–7.57 (m, 2H), 7.67–7.71 (m, 1H), 8.10–8.13 (m, 2H); ¹³C NMR (APT, 50 MHz, CDCl₃) δ (ppm) 121.2, 126.7, 129.0, 129.5, 129.7, 130.1, 132.3, 135.2, 149.8, 161.8, 185.2; MS *m/e* 51 (5.7), 77 (29), 105 (100), 198 (3.0), 226 (M⁺, 0.02). HRMS. Calcd for C₁₄H₁₀O₃: 226.0630. Measd: 226.0630. Spectroscopic data for EGPG: ¹H NMR (200 MHz, CDCl₃) δ (ppm) 4.74 (s, 4H),

Table 1. Initiators Studied

Acetophenone Derivatives		Phenylglyoxylate Esters	
Code	Structure	Code	Structure
Irgacure 651		MPG	
Irgacure 369		EPG	
Irgacure 184		PPG	
Irgacure 907		CEPG	
Irgacure 1700		BEPG	
Irgacure 500		SEPG	
Darocure 1173		EEPG	
Darocure 4265		EGPG	

7.45–7.52 (m, 4H), 7.60–7.68 (m, 2H), 7.79–8.03 (m, 4H); ^{13}C NMR (APT, 50 MHz, CDCl_3) δ (ppm) 62.9, 128.9, 130.0, 132.1, 135.1, 163.2, 185.5; MS m/e 51 (6.5), 77 (25), 105 (100), 178 (2.5), 326 (M^+ , 0.06). HRMS. Calcd for $\text{C}_{18}\text{H}_{14}\text{O}_6$: 326.0790. Measd: 326.0791.

Kinetic Measurements. TEGDA is one of the most common components of commercial photocurable systems and was selected as a typical monomer for testing the initiators. Solutions of each of the photoinitiators in TEGDA containing 0.1% (w/w) DASB were prepared. The concentrations of photoinitiators in the solutions used for the polymerizations were in the range $0.001\text{--}0.04\text{ M}^{-1}$ and adjusted appropriately so that the initial rate of polymerization, measured in terms of the fluorescence intensity ratio change, dI/dt , using a CM 1000 cure monitor^{12,17} did not exceed 0.025 s^{-1} , while being fast enough to achieve over 70% of the ratio span within 10 min. A 0.1-mm layer of each solution was prepared by squeezing a drop of the solution to be tested between glass slides ($75 \times 25 \times 1\text{ mm}$) separated by appropriate spacers, and a small spot on the layer was cured with the excitation beam of the CM 1000. The sample was placed directly on the sensor head of the CM 1000 and held in an upward position shielded from stray light by means of a dark box. Clamps on both edges held the glass slides together at a constant distance.

The fluorescence intensity ratio was measured at two monitoring wavelengths, 458 and 556 nm, selected¹² from the differences in the fluorescence intensities before and after full polymerization was achieved. The wavelength used for probe excitation and initiator activation was selected as 350 nm. Under such steady-state irradiation conditions, real-time kinetic profiles for TEGDA polymerization were obtained and relative kinetic parameters extracted from the curing profiles as described subsequently. All measurements were carried out at ambient temperature (about $23\text{ }^\circ\text{C}$). The kinetic profile for each of the initiators was repeated 3–5 times, and final values of the initiator efficiencies were averaged to obtain more accurate results as well as to evaluate the reproducibility of the technology.

Absorbance Measurements. The net absorbance of each photoinitiator at the wavelength used (350 nm) to polymerize the thin film (0.1 mm in thickness) was determined by preparing a separate standard solution of each initiator in TEGDA (i.e., the solutions without the probe) and measuring its absorption spectrum using pure TEGDA as the background. The absorbance at the wavelength of interest (350 nm) was read out from the UV absorption spectrum and the absorbance of the initiator in the thin film (0.1 mm in thickness) calculated as follows:

$$A = A_{\text{std}} \frac{m_i}{m_{i,\text{std}}} \frac{m_{\text{m, std}}}{m_{\text{m}}} \frac{l}{l_{\text{std}}} \frac{1}{\sin(60^\circ)}$$

A is the absorbance of the initiator in the 0.1 mm sample used for kinetic measurements, A_{std} is the absorbance of the initiator at the excitation wavelength (350 nm) in the standard solution in a cuvette of thickness l_{std} used in the UV measurement, m_i and $m_{i,\text{std}}$ are masses of the initiator in the sample solution (for thin film) and the standard solution (for UV measurement), respectively, m_{m} and $m_{\text{m, std}}$ are masses of the TEGDA monomer in the sample solution (for thin film) and the standard solution (for UV measurement), respectively, l is the thickness of the thin films ($l = 0.1$ mm), l_{std} is the thickness of the cuvette used in measuring the UV absorption spectrum of the standard solution ($l_{\text{std}} = 10$ mm), and $\sin(60^\circ)$ accounts for the 60° angle relative to the sample surface, at which the excitation light from CM 1000 passed through the sample (this is an intrinsic feature of the sensor head design of the CM 1000).

Determining the Relative Initiation Efficiency by FPT. The efficiency of a photoinitiating system can be described in terms of the quantum yield of initiation or the quantum yield of polymerization.²⁰ In this study, the initiation efficiency of the photoinitiator is expressed as the quantum yield of initiation and defined as the average number of polymer chains initiated by the initiator per photon absorbed. If one compares the performance of different photoinitiators in a particular monomer system, knowledge of absolute initiation efficiencies is unnecessary. Instead, one selects a common initiator as a reference and measures initiation efficiencies of other initiators relative to that of the reference. As the absolute initiation efficiency of the reference initiator in the monomer system selected becomes known, the relative initiation efficiencies of other initiators can be easily converted to absolute values as necessary. Therefore, in this study, the relative initiation efficiency (Φ_{rel}), defined as the ratio of the initiation quantum yield of any particular photoinitiator (Φ) to that of a reference photoinitiator (Φ_{ref}) (eq 1), was measured.

$$\Phi_{\text{rel}} = \Phi/\Phi_{\text{ref}} \quad (1)$$

The relative initiation efficiencies of the photoinitiators were determined from real-time kinetic curves according to the method below. In general, the kinetics of a free-radical polymerization can be described using classical equation (2)

$$R_p = k_p (R_i/k_t)^{1/2} [M] \quad (2)$$

where R_p is the rate of polymerization ($R_p = -d[M]/dt$), R_i is the rate of initiation, $[M]$ is the monomer concentration in the case of monofunctional monomers or the functional group concentration in the case of multifunctional monomers, and k_p and k_t are propagation and termination rate constants, respectively.

When polymerization is initiated by a photoinitiator under steady-state irradiation conditions, the rate of initiation is proportional to the initiation quantum yield of that initiator and to the amount of light absorbed by the sample (eq 3). The amount of the light absorbed can be calculated from eq 4.

$$R_i = \Phi_i \frac{\Delta I_{\text{abs}} S}{V} \quad (3)$$

$$\Delta I_{\text{abs}} = I_0 (1 - 10^{-A}) \quad (4)$$

is the initiation quantum yield, ΔI_{abs} is the amount of light absorbed by the initiator in the sample film, I_0 is the incident light intensity, for example, in $\text{einstein cm}^{-2} \text{ s}^{-1}$, S is the illuminated surface area, V is the illuminated volume, and A is the net absorbance of the initiator within the sample at the wavelengths used.

Substitution of eqs 3 and 4 into eq 2 yields general equation (5), which describes the photopolymerization kinetics in a thin

layer. Under identical irradiation and measurement condi-

$$R_p = k_p \sqrt{\frac{\Phi_i S I_0 (1 - 10^{-A})}{k_t V}} [M] \quad (5)$$

tions and for the same monomer, k_p , k_t , S , V , and I_0 are constant. Moreover, if the rate of polymerization is measured immediately after the induction period, where monomer conversion equals zero, the monomer concentration (functional group concentration for multifunctional monomers) is also constant (i.e., $[M] = [M]_0$). Under these conditions, eq 6 can be derived from eqs 1 and 5. As shown by eq 6, the relative

$$\Phi_{\text{rel}} = \left(\frac{R_{p0}}{R_{p0,\text{ref}}} \right)^2 \frac{1 - 10^{-A_{\text{ref}}}}{1 - 10^{-A}} \quad (6)$$

initiation efficiency (Φ_{rel}) of an initiator can be calculated from the absorbances and the initial rates of polymerization of this initiator and those of a reference. R_{p0} and $R_{p0,\text{ref}}$ are the initial rates of polymerization measured respectively for the photoinitiator of interest and the reference initiator and A and A_{ref} are the absorbances (in the film samples) of the photoinitiator of interest and the reference initiator, respectively.

Initial rates of polymerization (eq 6) can be expressed from the initial slopes of the kinetic curves describing functional group conversion as a function of time (eq 7) where α is the

$$R_{p0} = - \left(\frac{d[M]}{dt} \right)_{[M]=[M]_0} = [M]_0 \left(\frac{d\alpha}{dt} \right)_{\alpha=0} \quad (7)$$

functional group conversion ($\alpha = ([M]_0 - [M])/[M]_0$).

The kinetic profiles obtained by the FPT method represent the fluorescence intensity ratio, not the functional group conversion, as a function of time. To relate fluorescence intensity ratios to any other property, the relationship must be calibrated. Fluorescence intensity ratios are usually calibrated against functional group conversion and the resulting calibration curve used to convert the fluorescence ratio profile to the actual kinetic curve (functional group conversion profile).¹² This calibration curve is usually described by a polynomial (eq 8) relating the fluorescence intensity ratio (r)

$$r = r_0 + A_1 \alpha + A_2 \alpha^2 + \dots A_n \alpha^n \quad (8)$$

to the functional group conversion (α). Equation 9 can be derived from eqs 7 and 8 such that the initial rate of polymerization can be calculated directly from the initial slope of the fluorescence ratio (r) vs time (t) profile. r_0 is the the

$$R_{p0} = \frac{[M]_0}{A_1} \left(\frac{dr}{dt} \right)_0 \quad (9)$$

fluorescence intensity ratio before polymerization, A_1, \dots, A_n are the calibration coefficients found experimentally for a specific probe/monomer system, and $(dr/dt)_0$ is the initial slope of the kinetic profile obtained by the FPT method.

Substitution of eq 9 into eq 6 yields eq 10, which expresses

$$\Phi_{\text{rel}} = \frac{\left(\frac{dr}{dt} \right)_0^2 (1 - 10^{-A_{\text{ref}}})}{\left(\frac{dr}{dt} \right)_{0,\text{ref}}^2 (1 - 10^{-A})} \quad (10)$$

the relative initiation efficiency in terms of quantities that are directly measurable. Equation 10 was used to determine the relative initiation efficiencies of the initiators studied herein.

Extraction of Data from Kinetic Profiles Obtained by FPT. To determine precisely relative initiator efficiencies using eq 10, slopes of fluorescence ratio profiles at the starting point, where monomer conversion is zero, must be determined. The presence of polymerization inhibitors in commercial monomers causes a delay in the onset of polymerization (i.e.,

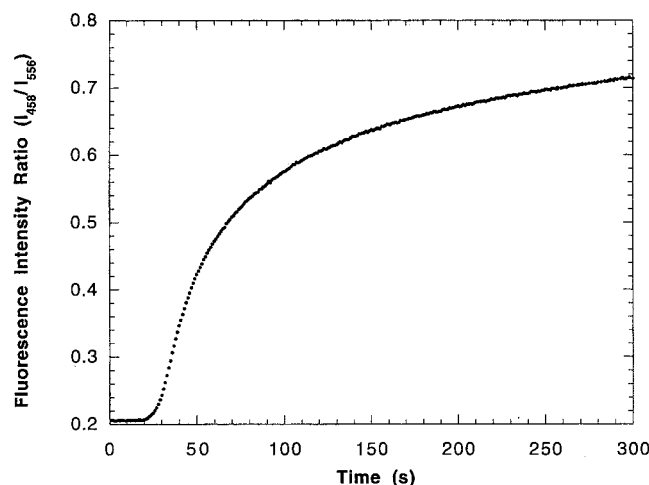


Figure 1. Example kinetic profile obtained by the FPT method for the polymerization of TEGDA initiated by Irgacure 651.

the polymerization does not start immediately after the light is turned on, and one always observes an induction period). During this period inhibitors are consumed by free radicals generated from the photoinitiator (Figure 1). Some residual inhibitor also remains during the initial stages of polymerization so the kinetic curve does not start sharply even when all but a small quantity of the inhibitors are consumed. Instead a smooth transition from the induction phase to the maximum polymerization rate phase is observed with a clear inflection point. Eventually, after most of the monomer is consumed, polymerization slows down and reaches a plateau. We propose the following two approaches to determine the initial dr/dt values needed in eq 10.

Kinetic Extrapolation Method. For the most precise measure of dr/dt values at zero monomer conversion, the initial portion of the kinetic profile needs to be extrapolated to $r = r_0$. This can be done by assuming first-order kinetics relative to functional group concentration for the initial portion of the polymerization curve. This is reasonable based on eq 5. Integration of eq 5 and conversion of the concentration ($[M]$) to functional group conversion (α) yields eq 11 where k_0 is the

$$-\ln(1 - \alpha) = k_0(t - t_0) \quad (11)$$

overall rate constant that includes all the quantities in eq 5 that are constant at low conversions and t_0 is the induction time.

Moreover, within a narrow range at low conversions (α relatively small) the calibration equation (eq 8) can be approximated as a linear relationship (eq 12).

$$r = r_0 + A_1\alpha \quad (12)$$

Substitution of α from eq 12 into eq 11 gives the equation that is used to extrapolate the kinetic data to zero conversion (eq 13) where r_m would be the final fluorescence ratio achieved

$$-\ln\left(1 - \frac{r - r_0}{r_m - r_0}\right) = k_0(t - t_0) \quad (13)$$

at the completion of the polymerization (i.e., for $\alpha = 1$) if first-order kinetics (eq 11) and the linearity of the calibration equation (eq 12) were obeyed over the entire range of polymerization.

Thus, by plotting $-\ln[1 - (r - r_0)/(r_m - r_0)]$ as a function of time, a straight line should be obtained within the range of conversions where eq 13 is followed. The initial slope of the original fluorescence ratio (vs time) profile at zero conversion is calculated from eq 14. Unfortunately, in this kinetic extrapolation method the parameter r_m is not known explicitly and have to be found by consecutive approximation until the

$$\left(\frac{dr}{dt}\right)_{r=r_0} = k_0(r_m - r_0) \quad (14)$$

relationship defined by eq 13 is obeyed (i.e., the plot of $-\ln[1 - (r - r_0)/(r_m - r_0)]$ vs time becomes a straight line). We used a loop within a spreadsheet program, which assumed consecutive values of r_m within an initially input range, and fit the experimental data to a linear regression based on eq 13 until the correlation coefficient did not increase by more than 0.000 01. Surprisingly, a perfectly linear match was obtained up to 50% of the fluorescence ratio span range. At values higher than 50%, no r_m value could be found that afforded a linear relationship based on eq 13. Hence, in the kinetic extrapolation method, we used data points in the range starting at the inflection point and ending in the middle (50%) of the ratio span, rather than going to higher conversions.

Figure 2 shows an example of the linear match obtained from the experimental data for Irgacure 907 using eq 13. Similar straight lines were also obtained for polymerizations initiated by other photoinitiators. In all the cases, the correlation coefficients for the linear match at the optimized r_m values were better than 0.9995. Moreover, the match quality was verified visually by plotting the corresponding graph to make sure that no data points within the range used for calculation were off the matched line.

Inflection Point Approximation. Instead of using the rate of photopolymerization at the start point, one can use the slope at the inflection point of the kinetic profile as an approximation for the rate of polymerization.²¹ This slope will always be somewhat smaller than the actual rate of polymerization measured at zero monomer conversion. Since we are more interested in the relative initiation efficiency (Φ_{rel}) rather than an absolute value, the ratio of polymerization rate of the sample initiator over that of the reference is more important than absolute rate values (cf. eq 10). The error in the rate ratio introduced by the inflection point approximation will be smaller than the error this introduces to the individual rate values. This is because, with such an approximation, the rate of the sample initiator and that of the reference are expected to deviate in the same direction from true values. Therefore, the relative initiation efficiency determined by the inflection point approximation is accurate enough for most applications. The slope at the inflection point can be easily determined by fitting the experimental data for the initial portion of the polymerization process (e.g., the portion from the start of polymerization at the end of the induction period up to the middle of the ratio span) into a high-order polynomial and finding the maximum value of the first-order derivative of that polynomial. We used a seventh-order polynomial which fit the initial portion of each kinetic profile (between the ratios 0.22 and 0.5) with a correlation coefficient better than 0.999 95.

Results and Discussion

This FPT method is based on monitoring the photopolymerization kinetics of a thin layer of monomer of interest using specially designed fluorescent probes as molecular sensors and a rapid scan fluorimeter to follow the changes in the probe fluorescence during the polymerization. By appropriate selection of the initiator concentration, the polymerization process occurs essentially under isothermal steady-state conditions. A monochromatic light is used as the irradiation source to carry out the photopolymerization in a small spot within the monomeric layer.

Following polymerization progress with a probe relies on measurements of shifts of the fluorescence spectrum of the probe to shorter wavelengths during the polymerization process.¹² The shift is measured as the fluorescence intensity ratio at two wavelengths selected on both sides of the maximum in the fluorescence spectrum. When the fluorescence intensity at a shorter wavelength is divided by the intensity at a longer

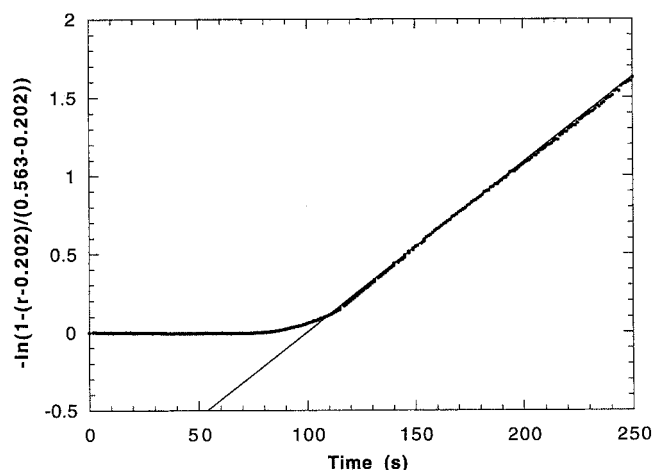


Figure 2. Example of a linearization of the kinetics profile of TEGDA polymerization initiated by Irgacure 907 using the kinetic extrapolation method.

wavelength, the resulting ratio increases monotonically as the reaction proceeds and becomes a quantitative indication of polymerization progress. By measuring the ratio using a rapid scan fluorimeter, hundreds of precise data points can be obtained within the polymerization period, and this allows recording of a real-time polymerization profile in terms of the fluorescence intensity ratios.

We used DASB as the probe in this study because of its good sensitivity in acrylate systems.¹² Figure 1 shows an example kinetic profile obtained for Irgacure 651 using the CM 1000 rapid scan cure monitor. In triethylene glycol diacrylate, the kinetic profile originated from a ratio of 0.21 (458/556 nm) before polymerization and reached a plateau at about 0.75 after sufficient photons were absorbed. This large span in the fluorescence intensity ratio (i.e., over a 3-fold change) afforded sufficient resolution to measure the kinetic data precisely. Similar kinetic curves were obtained for other initiators.

By using appropriate spacers, we were able to keep the thickness of the monomer layer between the glass slides fixed at about 0.1 mm. It is important to keep a constant spacing between the slides so that the thickness of the monomer film does not vary from run to run. We found that using paper spacers caused up to 10% error in the kinetic profiles so more rigid spacers (possibly made of copper or aluminum) are recommended for more accurate results. Moreover, it is important to keep the light intensity and the temperature constant in all the experiments for kinetic comparisons. In this study, the measurements were carried out in a temperature-controlled room. The CM 1000 cure monitor was allowed to warm for at least 1 h before the kinetic measurements were obtained to ensure constancy of the light intensity during the experiments. The stability of the measurement conditions can be verified by recording the kinetic profile of a reference initiator solution at the beginning and the end of a series of experiments. These profiles should be identical.

The illuminated area provided by the CM 1000 cure monitor sensor head was about 5 mm in diameter. The reaction volume was quite low, on the order of 2 μ L. The relatively large surface area and small sample thickness allowed efficient dissipation of the heat released during the polymerization process. Thus, polymerization rates were measured under reaction

conditions that were practically isothermal. If conditions are selected such that the polymerization is finished within a few seconds, the heat produced by the polymerization is not able to dissipate rapidly and the reaction temperature could increase as a result. Changes in reaction temperature influence polymerization rate, and measurements carried out under such conditions do not reflect true reactivities of the initiator.²² We therefore adjusted the initiator concentration such that the initial slope, dr/dt , did not exceed 0.02 s^{-1} for 0.1-mm-thick samples. In general, the thicker the sample, the slower the polymerization should be to preserve isothermal conditions.

Another advantage that polymerization in a thin layer afforded is the uniformity of the illumination in the reaction media. The absorbance of an initiator in the 0.1-mm layer at the illumination wavelength was on the order of 0.005–0.08, depending on the initiator. We found that, at higher absorbances, the polymerization kinetics became too fast for reliable measurements. Meanwhile, the small absorbance minimized the gradient of light intensity across the sample thickness. For example, at the absorbance of 0.08, the illumination intensity at the back surface of the sample is only 20% lower than that at the front surface. This makes the steady-state concentration of free radicals uniform within the volume illuminated.

We squeezed a drop of the monomer between two glass slides to form a monomer layer and made measurements at a spot in the center of this layer. This allowed measurement of polymerization kinetics under anaerobic conditions—an important factor since oxygen is known to inhibit free-radical polymerization. Were the solution not free from contact with air during the measurement, we found that the kinetics were affected. At 0.1-mm layer thickness, the diffusion of oxygen to the reacting spot through the monomer layer is negligible. Traces of oxygen dissolved in monomer within the illuminated area (including any other inhibitors present in the monomer) are consumed during the induction period observed in the kinetic profile.

Light of any reasonable wavelength can be used to excite the photoinitiator being tested, provided that the initiator shows some absorption at the wavelength selected. However, the same wavelength should also be used to excite the reference initiator because the intensity of a light source usually varies with wavelength. Using a monochromatic light for the polymerization permits an accurate measurement of the amount of light absorbed by the sample. This is achieved by determining the absorbance of the initiator at that wavelength. If a broad-band excitation source is used, one has to integrate the absorption spectrum over the wavelength range to calculate the number of photons absorbed by the initiator. Variation in intensity of the irradiation light source along these wavelengths also has to be taken into account, which, in turn, requires knowledge of the exact energy distribution of the light source. Furthermore, eq 10 becomes more complex for excitation with polychromatic light. After absorbing photons from the light source, initiator molecules are promoted to their excited states, which, in turn, convert to the lowest vibrational level before any photoreaction happens. Thus, it does not matter which wavelength is used for excitation as long as the corresponding photon energy is above the $E^{0,0}$ energy level of the excited state of the initiator involved. In the case of a

Table 2. Initiation Efficiency of Various Commercial UV Photoinitiators Relative to Irgacure 651 in TEGDA Monomer

initiator	relative efficiency	
	kinetic extrapolation	inflection point approximation
unimolecular initiator		
Irgacure 369	1.42 ± 0.08^a	1.57 ± 0.05^a
Irgacure 651 (reference)	1	1
Darocure 1173	0.73 ± 0.02^a	0.88 ± 0.03^a
Irgacure 184	0.23 ± 0.01^a	0.28 ± 0.02^a
Irgacure 907	0.18 ± 0.01^a	0.22 ± 0.02^a
mixture initiators		
Irgacure 1700	1.14 ± 0.06^a	1.31 ± 0.04^a
Darocure 4265	0.75 ± 0.04^a	0.98 ± 0.05^a
Irgacure 500	0.13 ± 0.03^a	0.17 ± 0.04^a

^a Standard deviations (σ_{n-1}).

mixture of photoinitiators of differing absorption characteristics, relative initiation efficiencies, as determined by the FPT method using a monochromatic light source, must be treated with caution. The efficiency of photopolymerizations using a mixture is likely to depend on several factors, such as which of the components of the mixture absorbs light at the wavelength used for excitation and to what extent. Therefore, the results reported in Table 2 for Irgacure 1700, Darocure 4265, and Irgacure 500 are limited only to a comparison of efficiencies at 365-nm excitation. The results for the other initiators studied can be expected to be wavelength independent.

The relative efficiencies determined by kinetic extrapolation seem to be more reproducible (i.e., there is less relative error) than data obtained from the inflection point approximation and are a little lower than those from the later method. However, trends in the variation of the efficiency between the various initiators are exactly the same for results derived using both methods. This means that, for comparison of relative initiation efficiencies (as in the case of optimization of the initiator structure in the design of new photoinitiators), either method can be used as long as it is used consistently. The method based on the inflection point slope is preferred because it is easier to apply (i.e., the slope at the inflection point can be even found by plotting a graph and drawing the tangent line at that point with a ruler, though such a primitive method would not be very accurate). The kinetic extrapolation method is more sophisticated and requires some macro programming. It turned out that even though the correlation coefficient achieved for line matching was usually better than 0.9995 when about 100 data points were used; the corresponding initial slope varied slightly (i.e., by a few percent) depending on how wide a range in the ratios (i.e., how many data points) was taken for the extrapolation. Therefore, even when the kinetic extrapolation method is used for data workup, averaging the slopes from several independent measurements for the same initiator is recommended for maximum accuracy. We recommend that the kinetic extrapolation method be used only for cases where absolute initiation quantum efficiencies of a series of photoinitiators need to be determined precisely in a particular monomer system from a known absolute efficiency value of a reference initiator. The relative efficiencies determined by the inflection point method may be off by several percent from the true physically meaningful value. For relative comparisons of photoinitiator performance, the inflection point method is more practical.

Table 3. Relative Initiation Efficiency of Phenylglyoxylate Derivatives

initiator	relative efficiency	
	kinetic extrapolation	inflection point approximation
PPG	0.080 ± 0.004^a	0.096 ± 0.007^a
SEPG	0.12 ± 0.01^a	0.16 ± 0.003^a
MPG	0.26 ± 0.01^a	0.38 ± 0.02^a
EPG	0.26 ± 0.02^a	0.29 ± 0.04^a
CEPG	0.30 ± 0.02^a	0.40 ± 0.03^a
BEPG	0.30 ± 0.01^a	0.37 ± 0.02^a
EEPG	0.29 ± 0.02^a	0.38 ± 0.02^a
EGPG	not determined	0.38 ± 0.01^a

^a Standard deviations (σ_{n-1}).

The relative initiation efficiencies for the initiators studied, determined by both data workup methods, are summarized in Tables 2 and 3. The data in Table 2 indicate that, among the commercial photoinitiators studied, relative efficiencies vary from 1.42 for the Irgacure 369 to 0.18 for Irgacure 907. Thus, the selection of the proper photoinitiator is critical for each specific monomer system. For example, in triethylene glycol diacrylate, Irgacure 369 initiates 7 times more polymer chains than does Irgacure 907 when the same amount of photons were absorbed!

Low initiator efficiency may result from several factors intrinsic to initiator structure: (1) loss of excitation energy by fluorescence or internal conversion to the ground state, prior to bond cleavage; (2) side reactions of the excited state that do not generate free radicals such as bimolecular quenching; (3) the radicals derived from photolysis not being reactive enough, thus leading only to radical recombination or primary radical termination of growing polymer chains, etc. Therefore, the FPT method provides an effective tool for comparing the performances of different initiators, and this, in turn, enables the selection of the optimum photoinitiator for a given system as well as the design of improved initiators.

MPG has been sold as a commercial photoinitiator since the late 1960s, and the radical chain initiation mechanism resulting from its photolysis was recently studied.²³ Since we have had a long-standing interest in the photochemistry of phenylglyoxylates,²⁴ we also applied the FPT method in a systematic study of several initiators derived from phenylglyoxylic acid.¹⁹ Relative initiator efficiencies referenced to Irgacure 651 in TEGDA are collected in Table 3.

Intermolecular hydrogen abstraction, the reaction that results in initiation with the parent compound MPG,²³ is not possible with PPG because of the absence of abstractable hydrogens in the compound. In aprotic solvents, the photolysis of PPG is dominated by photo-Fries rearrangement.²⁵ The limited initiator function which does result from PPG derives from benzoyl radicals that escape the solvent cage during the photo-Fries rearrangement. EPG reacts, formally, in a way similar to that of MPG so their initiation efficiencies are comparable. In addition to the hydrogen abstraction reactions common in both MPG and EPG, β -cleavage from the intermediate 1,4-biradical derived from Norrish type II reaction is also observed when BEPG, CEPG, and SEPG are irradiated.^{19b} This accounts for the slightly higher efficiencies for BEPG and CEPG as compared to MPG. In contrast the efficiency of SEPG is lower than that of MPG. β -Cleavage dominates the reaction of SEPG and produces the stable phenylthio

radical,^{19b} which couples with other radicals produced in the system, thus reducing the overall initiation efficiency. The efficiencies of EEPG and EGP are not significantly better than that of MPG even though more reactive hydrogens (those α to the ether oxygen) are available in EEPG.

Conclusions

Application of fluorescence probe technology and a rapid scan fluorimeter afforded a facile and precise method for relative comparison of the initiator efficiency of various free-radical photoinitiators. The FPT method provides a tool for evaluation of relative initiation efficiencies of new photoinitiators, which can be used to optimize the initiator structure.

The initiation efficiencies of phenylglyoxylate derivatives vary with structure. This is understood by the changes in photoreaction patterns associated with the structural modifications. Work in the design and synthesis of better performing phenylglyoxylate derivatives is underway in this laboratory.

Acknowledgment. This work was supported the National Science Foundation (DMR-90113109) and the Office of Naval Research (N00014-93-1-0772). Conversations with Dr. G. S. Hammond are gratefully acknowledged. S.H. thanks Spectra Group Limited for hosting him during this study and for the use of the CM 1000 cure monitor. R.P. acknowledges a postdoctoral fellowship at BGSU/SGL.

References and Notes

- (1) Contribution No. 353 from the Center for Photochemical Sciences.
- (2) Fouassier, J.-P. *Photoinitiation, Photopolymerization, and Photocuring: Fundamentals and Applications*; Hanser Publishers: Cincinnati, OH, 1995.
- (3) Decker, C.; Moussa, K. *Makromol. Chem.* **1988**, *189*, 2381.
- (4) Maihot, G.; Bolte, M. *J. Photochem.* **1991**, *56*, 387.
- (5) Decker, C.; Moussa, K. *Macromolecules* **1989**, *22*, 4455.
- (6) Schweri, R. *J. Radiat. Curing* **1991**, *1*, 36.
- (7) Decker, C.; Moussa, K. *J. Coat. Technol.* **1990**, *62*, 55.
- (8) Davidson, R. S.; Lowe, C. *Eur. Polym. J.* **1989**, *25*, 159.
- (9) Kloosterboer, J. G.; Van de Hei, G. M. M.; Boots, H. M. J. *Polym. Commun.* **1984**, *25*, 354.
- (10) Carlini, C.; Rolla, P. A.; Tombari, E. *J. Appl. Polym. Sci.* **1990**, *41*, 805.
- (11) Carre, C.; Lounnot, D. J.; Fouassier, J. P. *Macromolecules* **1989**, *22*, 791.
- (12) (a) Paczkowski, J.; Neckers, D. C. *Macromolecules* **1991**, *24*, 3013. (b) Popielarz, R.; Neckers, D. C. *Proc. RadTech North America* **1996**, 271. (c) Eckberg, R. P.; Marino, T. L.; Popielarz, R.; Neckers, D. C. *Proc. RadTech North America* **1996**, 399.
- (13) Song, J. C.; Torres-Filho, A.; Neckers, D. C. *Proc. RadTech North America* **1994**, 338.
- (14) Valdez-Aguilera, O.; Pathak, C. P.; Neckers, D. C. *Macromolecules* **1990**, *23*, 689.
- (15) Paczkowski, J.; Neckers, D. C. *Chemtracts: Macromol. Chem.* **1992**, *3*, 75.
- (16) Jager, W. F.; Volkers, A. A.; Neckers, D. C. *Macromolecules* **1995**, *28*, 8153.
- (17) CM 1000 is available from Spectra Group Ltd., Inc., 1722 Indian Wood Circle, Suite H, Maumee, OH 43537.
- (18) IUPAC names of commercial photoinitiators: Irgacure 651, 2,2-dimethoxy-2-phenylacetophenone; Irgacure 369, 2-benzyl-2-(*N,N*-dimethylamino)-1-(4-morpholinophenyl)-1-butanone; Irgacure 184, 1-hydroxycyclohexyl phenyl ketone; Irgacure 907, 2-methyl-1-[4-(methylthio)phenyl]-2-morpholinopropan-1-one; Irgacure 1700, bis(2,6-dimethoxybenzoyl)-2,4,4-trimethylpentylphosphine oxide & 2-hydroxy-2-methyl-1-phenylpropan-1-one; Irgacure 500, 1-hydroxycyclohexyl phenyl ketone benzophenone; Darocure 1173, 2-hydroxy-2-methyl-1-phenylpropan-1-one; Darocure 4265, 2-hydroxy-2-methyl-1-phenylpropan-1-one & (2,4,6-trimethylbenzoyl)diphenylphosphine oxide.
- (19) (a) Hu, S.; Neckers, D. C. *Tetrahedron* **1997**, *53*, 2751. (b) Hu, S.; Neckers, D. C. *J. Org. Chem.* **1997**, *62*, 7827.
- (20) Fouassier, J.-P. In *Radiation Curing in Polymer Science and Technology*; Fouassier, J.-P., Rabek, J. F., Eds.; Elsevier: London, 1993; Vol. 1.
- (21) This approximation was usually taken for granted; i.e., the slope at inflection point was commonly taken as the rate of polymerization; for example, see ref 3.
- (22) In this respect, the reactivity measurements under laser irradiation (fast polymerization) were not the intrinsic reactivities of the initiators.
- (23) Hu, S.; Neckers, D. C. *J. Mater. Chem.* **1997**, *7*, 1737.
- (24) Huyser, E. S.; Neckers, D. C. *J. Org. Chem.* **1964**, *29*, 276.
- (25) Hu, S. Ph.D. Dissertation, Bowling Green State University, Bowling Green, OH, 1998.

MA971390L